MCB
Journals.ASM.org

Alternative Splicing Shapes the Phenotype of a Mutation in *BBS8* To Cause Nonsyndromic Retinitis Pigmentosa

Daniel Murphy,[a] Ratnesh Singh,[b] Saravanan Kolandaivelu,[b] Visvanathan Ramamurthy,[a,b,c] Peter Stoilov[a]

Departments of Biochemistry[a] and Ophthalmology[b] and Center for Neuroscience,[c] Robert C. Byrd Health Sciences Center, West Virginia University, Morgantown, West Virginia, USA

Bardet-Biedl syndrome (BBS) is a genetic disorder affecting multiple systems and organs in the body. Several mutations in genes associated with BBS affect only photoreceptor cells and cause nonsyndromic retinitis pigmentosa (RP), raising the issue of why certain mutations manifest as a systemic disorder whereas other changes in the same gene affect only a specific cell type. Here, we show that cell-type-specific alternative splicing is responsible for confining the phenotype of the A-to-G substitution in the 3′ splice site of *BBS8* exon 2A (IVS1-2A>G mutation) in the *BBS8* gene to photoreceptor cells. The IVS1-2A>G mutation leads to missplicing of *BBS8* exon 2A, producing a frameshift in the *BBS8* reading frame and thus eliminating the protein specifically in photoreceptor cells. Cell types other than photoreceptors skip exon 2A from the mature *BBS8* transcript, which renders them immune to the mutation. We also show that the splicing of *Bbs8* exon 2A in photoreceptors is directed exclusively by redundant splicing enhancers located in the adjacent introns. These intronic sequences are sufficient for photoreceptor-cell-specific splicing of heterologous exons, including an exon with a randomized sequence.

The BBSome is a multiprotein complex that is thought be required for the transport of proteins in and out of the cilia. The BBSome interacts with intraflagellar transport A (IFT-A) and IFT-B complexes and promotes the assembly of the IFT machinery (1–7). Several proteins, such as the G-protein-coupled receptors Smo, Sstr3, Mchr1, and Vipr2, depend on the BBSome for their ciliary transport, suggesting a possible role for the BBSome as an adapter that connects the IFT complex to its cargo in primary cilia (2, 8, 9). Mutations in genes that encode BBSome components and proteins associated with the BBSome are linked to systemic Bardet-Biedl syndrome (BBS). BBS is an autosomal recessive ciliopathy caused by defects in the BBSome that disrupt the normal ciliary function throughout the body. BBS symptoms include retinitis pigmentosa (RP), skeletal malformations, mental retardation, obesity, hearing impairment, shortened limbs, polydactyly, and kidney cysts (10, 11). In photoreceptor cells, BBSome deficiency leads to defects in rod outer-segment formation and localization of rod opsin and, ultimately, photoreceptor cell death (10–13). The severity of the BBS symptoms can vary considerably due to the nature of the mutation and the genetic background. Interestingly, phenotypes of different mutations in the same gene can range from a classical BBS that affects multiple systems to nonsyndromic RP, where the phenotype is limited to loss of photoreceptor function. For example, the *ARL6* (*BBS3*) A89V, *BBS1* M390R, and *BBS8* IVS1-2A>G mutations cause nonsyndromic RP, while several other mutations in the same genes manifest as classical BBS, presenting additional symptoms such as obesity, hearing impairment, polydactyly, and mental retardation in addition to the loss of vision (7, 14–19). The existence of BBSome mutations that cause nonsyndromic RP is interpreted to indicate a specific function for this protein complex in vision. This hypothesis is further supported by the requirement for the Arl6 long (Arl6L) splice isoform that is specific to the retina for photoreceptor survival (20, 21).

BBS8 is a tetratricopeptide repeat (TPR) protein that is part of the core BBSome particle. BBS8 was recently shown play a role in establishing planar cell polarity and orientation of cilia in epithelial cells (22). To date, six mutations in the *BBS8* gene have been linked to classical BBS (18, 23, 24). An exception to this pattern is the *BBS8* IVS1-2A>G mutation, which disrupts the 3′ splice site of *BBS8* exon 2A and causes nonsyndromic RP. It was postulated that the IVS1-2A>G mutation induces skipping of the exon to produce a shorter splice variant (BBS8S) (19). The long form of *BBS8* containing the 30-nucleotide (nt) exon 2A (BBS8L) is detected exclusively in the photoreceptor outer nuclear layer (ONL) but not in other parts of the retina which express the short BBS8S isoform (19). Analogous to Arl6, where the Arl6L splicing isoform is needed for photoreceptor survival, it was proposed that the RP phenotype is due to the inability of BBS8S protein to substitute for a crucial function performed by the longer BBS8L isoform in photoreceptor cells (19–21).

Here, we show that *BBS8* exon 2A is highly photoreceptor specific. We dissected the sequences that direct Bbs8 exon 2A splicing and show that splicing enhancers within the flanking introns are sufficient to drive photoreceptor-specific inclusion of exon 2A and unrelated exons. The mechanisms controlling the cell-type-specific splicing of *BBS8* exon 2A modify the phenotype of the IVS1-2A>G mutation to eliminate the BBS8 protein specifically in photoreceptors and cause nonsyndromic RP.

Received 13 January 2015 **Returned for modification** 14 February 2015
Accepted 10 March 2015

Accepted manuscript posted online 16 March 2015

Citation Murphy D, Singh R, Kolandaivelu S, Ramamurthy V, Stoilov P. 2015. Alternative splicing shapes the phenotype of a mutation in *BBS8* to cause nonsyndromic retinitis pigmentosa. Mol Cell Biol 35:1860–1870. doi:10.1128/MCB.00040-15.

Address correspondence to Visvanathan Ramamurthy, ramamurthyv@wvuhealthcare.com, or Peter Stoilov, pstoilov@hsc.wvu.edu.

Supplemental material for this article may be found at http://dx.doi.org/10.1128/MCB.00040-15.

doi:10.1128/MCB.00040-15

MATERIALS AND METHODS

Mice. The procedures used in this work were approved by Institutional Animal Care and Use Committee at West Virginia University (WVU). The *in vivo* subretinal injection and electroporation experiments were carried out in CD-1 mice (Charles River). The interacting protein-like 1 (*Aipl1*) and *Nrl* knockouts were described previously (25, 26). *Nrl* knockouts were a generous donation from Anand Swaroop (NEI). The two knockout alleles were maintained in the C57BL/6J genetic background (Jackson Laboratory, Bar Harbor, ME).

RNA isolation and RT-PCR. Mouse eyes were enucleated at postnatal day 16 (P16) and dissected under a microscope (Zeiss Stemi DV4) to isolate the retina. Retinal RNA was isolated with Tri reagent (Sigma) according to the manufacturer's guidelines. Reverse transcription-PCR (RT-PCR) mixtures containing 0.1 to 0.5 μg RNA were primed with oligo(dT) and random hexamers to generate cDNA. The alternatively spliced regions were amplified using fluorescently labeled primers (listed in Table S2 in the supplemental material) positioned in the flanking constitutive exons (27). The amplified products were separated by gel electrophoresis under denaturing conditions (urea/polyacrylamide gels) and imaged on a Typhoon 9410 imager (GE). The band intensities on the gels were quantified using ImageQuant software (GE). For sequencing, the PCR products were isolated from agarose gels, purified using a QIAquick gel extraction kit (Qiagen), and either sequenced directly or cloned into pGEM T-Easy vector (Promega) prior to sequencing.

Real-time PCR. *Rho*, *Opn1sw*, *Gnat1*, *Gnat2*, *Pde6a*, and *Pde6c* expression was quantified by SYBR green quantitative PCR (qPCR). The expression of each gene was normalized to the average expression of three reference genes: *GusB* (encoding β-glucuronidase), *ActB* (encoding β-actin), and *Gapdh* (encoding GAPDH [glyceraldehyde-3-phosphate dehydrogenase]). See Table S2 in the supplemental material for primer sequences.

Antibodies. The *Bbs8* exon 2A antiserum was produced by Pacific Immunology. The serum was raised in rabbits against a peptide antigen (C-SPYDQEPAPDLPVSQA) that corresponds to the mouse exon 2A and includes six amino acid residues from the flanking exons to improve its immunogenicity. The antibody was affinity purified using the antigen peptide coupled to SulfoLink resin (Pierce). We also used the following commercial antibodies: pan-Bbs8 rabbit polyclonal antibody E-2 (Santa-Cruz Biotech) and GAPDH mouse monoclonal antibody 10RG109a (Fitzgerald). The antibodies to Pdc, Chx, and Pax6 were kind gifts from Maxim Sokolov and Peter Mathers (WVU).

Western blotting. Flash frozen retinal samples ($Aipl1^{+/+}$ and $Aipl1^{-/-}$) and lysates of N2A cells transiently transfected with *BBS8*-expressing construct were homogenized by sonication (Microson Ultrasonic cell disruptor) in 1× phosphate-buffered saline (PBS) containing protease inhibitors (Roche Complete). The protein concentration was measured by using a NanoDrop spectrophotometer (ND-1000; Thermo Scientific). Equal concentrations (150 μg) of protein samples were resolved in 10% SDS-PAGE gel electrophoresis and then transferred to an Immobilon-FL membrane (Millipore). Membranes were incubated with blocking buffer (Rockland) for 30 min at room temperature. After blocking, membranes were incubated with primary anti-Bbs8 antibodies at a 1:1,000 dilution for 4 h at room temperature. The secondary antibodies, Odyssey goat anti-rabbit antibody–Alexa Fluor 680 and Odyssey goat anti-mouse antibody–Alexa Fluor 680 (Li-COR Biosciences), were used at a 1:50,000 dilution for 30 min at room temperature. Membranes were scanned using an Odyssey infrared imaging system (Li-COR Biosciences).

Retinal tissue sections and fluorescence imaging. Mouse eyes were enucleated at P20 and incubated in 4% paraformaldehyde for 10 min. After removal of the cornea, the dissected eye was incubated in 4% paraformaldehyde for an additional 1 h with shaking. After three 5-min washes in PBS, the eye were cryoprotected by shaking at 4°C overnight in PBS containing 20% sucrose. Eyes were then incubated for 1 h with shaking in a 1:1 mixture of optimal cutting temperature (OCT) (Tissue Tek) compound and 20% sucrose–PBS, during which time the lens was removed. Eye cups were then flash frozen in OCT compound and stored at −80°C. Retinal sections (16 μm thick) were cut (Leica CM1850) and mounted on Superfrost Plus (Fisher) slides and stored at −20°C. Slides were washed in PBS to remove excess OCT compound and mounted with Prolong Gold reagent containing DAPI (4′,6-diamidino-2-phenylindole) (Life Technologies). The slides were imaged on a Zeiss LSM 510 laser scanning confocal microscope.

Generation of minigenes. The *Bbs8* exon 2a minigene was created by inserting a 700-bp fragment containing Bbs8 exon 2a and surrounding intron sequences into the EcoRI and BamHI sites of pFLare9a. The Bbs8 site-directed mutagenesis was performed using PCR overlap extension. The sequences of the primers used for cloning are in Table S2 in the supplemental material. The construction of Dup 51 and Dup 34 exon minigenes was described in our earlier publication (28).

Modification of BAC clones. The RP11-99F24 bacterial artificial chromosome (BAC) clone carrying the full-length human *BBS8* gene was purchased from the BACPAC Resources Center at Children's Hospital Oakland Research Institute (Oakland, CA) and verified by end sequencing and restriction fragment analysis. The IVS1-2A>G mutation and the tandem Flag-hemagglutinin tag at the C terminus of the product of the *BBS8* open reading frame (ORF) were introduced into the RP11-99F24 BAC clone using recombineering following previously described procedures (29). Restriction digests and sequencing of the targeted sites were used to ensure that the expected recombination events had occurred without unintended changes in the surrounding sequences.

Subretinal injection and electroporation. Minigene plasmid DNA was isolated at 4 to 7 μg/μl using a Qiagen Plasmid Plus Midi kit. DNA containing 0.1% fluorescein sodium was injected into the subretinal space of newborn CD-1 pups as described previously (30). Briefly, after anesthesia, an incision was made at the future eyelid with a 33-gauge needle under a dissecting microscope. The needle was used to make a pinhole puncture in the sclera away from the lens. A 0.5-μl volume of DNA was injected through the puncture into the subretinal space using a blunt-end syringe. Five pulses of 80 V of 50-ms duration with 950-ms intervals were then applied with tweezer-type electrodes (BTX model 520) (7-mm diameter). All experimental results and conclusions are based on at least three independent experiments (see Table S1 in the supplemental material for the number of replicates used in each experiment).

RESULTS

The long form of BBS8 (BBS8L) is predominantly expressed in photoreceptor cells. A previous study analyzing *Bbs8* messages from various retinal layers obtained by laser-captured microdissection showed that exon 2A is included in the photoreceptor layer. It was unclear if exon 2A inclusion in the mature *Bbs8* transcripts is a general feature of photoreceptor cells or if it is restricted to rods, which comprise 97% of the mouse retina. We first established the tissue specificity of exon 2A inclusion using RT-PCR to analyze the splicing of *Bbs8* in various mouse tissues. Other than the retina, we did not observe significant exon 2A inclusion in any of the tissues that we examined (Fig. 1A and B). Low levels of exon 2A inclusion were detected in the cortex and cerebellum after overexposing the gel with the RT-PCR products (Fig. 1A, lower panel).

To confirm that exon 2A-containing transcripts in the retina are specific to photoreceptor cells, we analyzed *Bbs8* splicing in the retina of Aryl hydrocarbon receptor interacting protein like-1 (*Aipl1*) knockout mice at P60 and compared the results to those determined with age-matched littermates. *Aipl1* is required for photoreceptor cell survival. Consequently, the retina of *Aipl1* knockout mice lacks photoreceptor cells by P30 but retains the inner neurons and retinal pigmented epithelium (25). RT-qPCR analysis of the expression of cone and rod photoreceptor markers

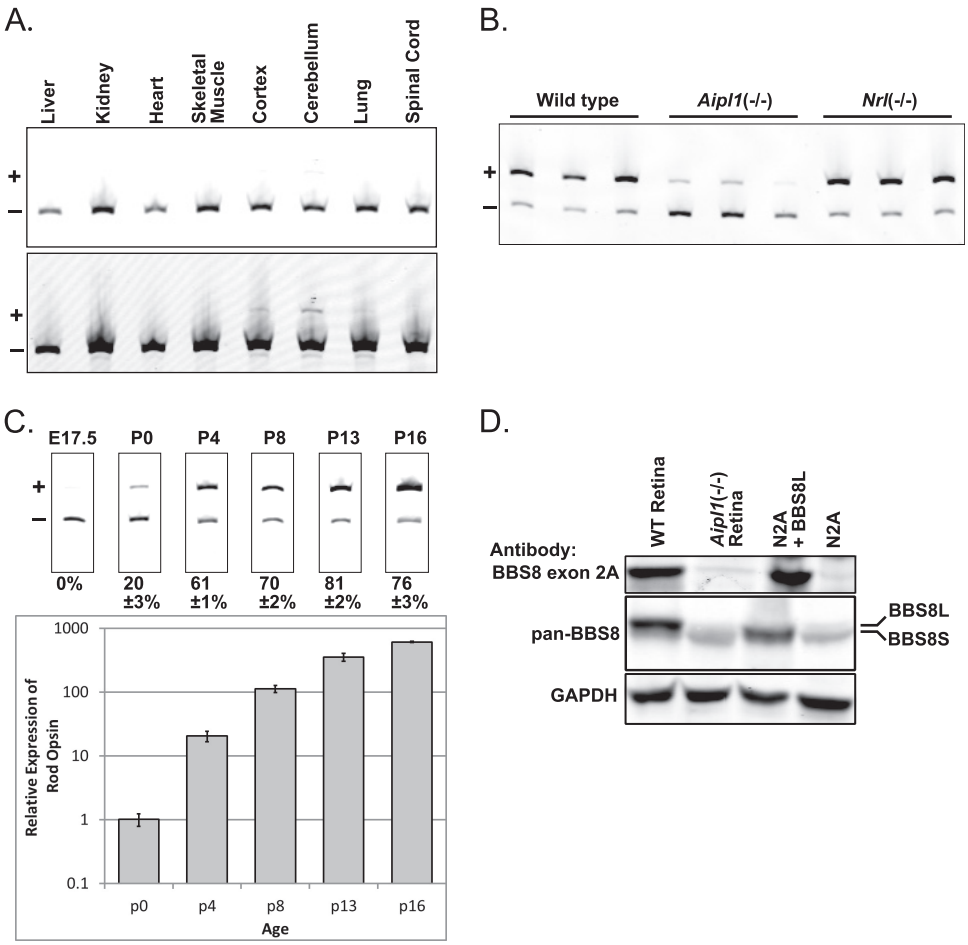

FIG 1 *Bbs8* transcripts containing exon 2A are specifically expressed in photoreceptor cells. (A) *Bbs8* exon 2A splicing was analyzed by RT-PCR in a panel of mouse tissues. Exon 2A was skipped or included at very low levels in all of the tissues we examined ("+" and "−" indicate exon inclusion and skipping, respectively). Some exon 2A inclusion was detected after overexposing the gel (panel below) in neural tissues from wild-type animals. (B) RT-PCR analysis of *Bbs8* exon 2A splicing in the retina of wild-type, *Aipl1* knockout, and *Nrl* knockout animals. Exon 2A was included at high levels in the retina of wild-type and *Nrl* knockout mice and was largely skipped in the retina of the *Aipl1* knockout mice. (C) Exon 2A inclusion in the mature *Bbs8* transcript was first detected at postnatal day 0 (left) and increased rapidly thereafter. The increase in exon 2A inclusion correlates with the increase in rod opsin expression as detected by quantitative RT-PCR (qRT-PCR) (right). (D) Protein extracts from wild-type (WT) mouse retina cells, Aipl1 knockout retina cells, N2A cells transfected with BBS8L expression, and mock-transfected N2A cells were probed with rabbit polyclonal antibody raised against a peptide antigen containing the exon 2A sequence (top) and a pan-BBS8 antibody (bottom). The BBS8L protein, recognized specifically by the anti-exon 2A antibody, was not detected in the mock-transfected N2A cells and was lost in the Aipl1 knockout retina. Similarly, low levels of the BBS8S protein were detected by the pan-BBS8 antibody in Aipl1 knockout retina and mock-transfected N2A cells.

(*Opn1sw*, *Gnat2*, *Pde6c*, *Rho*, *Gnat1*, and *Pde6a*) in the *Aipl1* knockout retina confirmed that there were few if any photoreceptor cells left (see Fig. S1 in the supplemental material). We reasoned that if *Bbs8* exon 2A is expressed exclusively in photoreceptor cells, we should see a dramatic reduction in its inclusion in *Aipl1* knockout animals compared to wild-type littermates. In agreement with a previous study characterizing *Bbs8* exon 2A splicing, we found that expression of the *Bbs8L* isoform was severely reduced in the retina of the adult *Aipl1* knockout animals (Fig. 1B) (19). This result demonstrates that exon 2A is included in the mature *Bbs8* RNA in photoreceptor cells. To determine if *Bbs8* exon inclusion is specific to a particular photoreceptor cell type in the retina, we compared the splicing of the *Bbs8* transcripts in retina from wild-type mice to retina from mice lacking the *Nrl* transcription factor. The retina of the *Nrl* knockout animal is enriched in cones and lack rods (26). RT-qPCR analysis of the expression of photoreceptor-specific genes confirmed elevated expression of cone markers (*Opn1sw*, *Gnat2*, and *Pde6c*) and loss of rod markers (*Rho*, *Gnat1*, and *Pde6a*) in the retina of *Nrl* knockout mice (see Fig. S1). The level of exon 2A inclusion in the retina of the *Nrl* knockout mouse was indistinguishable from that in the wild-type mouse retina (Fig. 1B), indicating that rods and cones include *Bbs8* exon 2A.

We next examined the splicing of *Bbs8* exon 2A in the course of retinal development. Inclusion of exon 2A was not detectable in the retina at embryonic day 17.5 (E17.5). Exon 2A was detected first at postnatal day 0 (P0), and its inclusion increased rapidly thereafter (Fig. 1C). This change in exon 2A inclusion levels closely correlates with photoreceptor outer-segment morphogenesis as well as expression of rod opsin, which is not detectable at E17.5 and rapidly rises after birth (Fig. 1C) (31). Thus, the developmental regulation of exon 2A splicing and its splicing pattern in

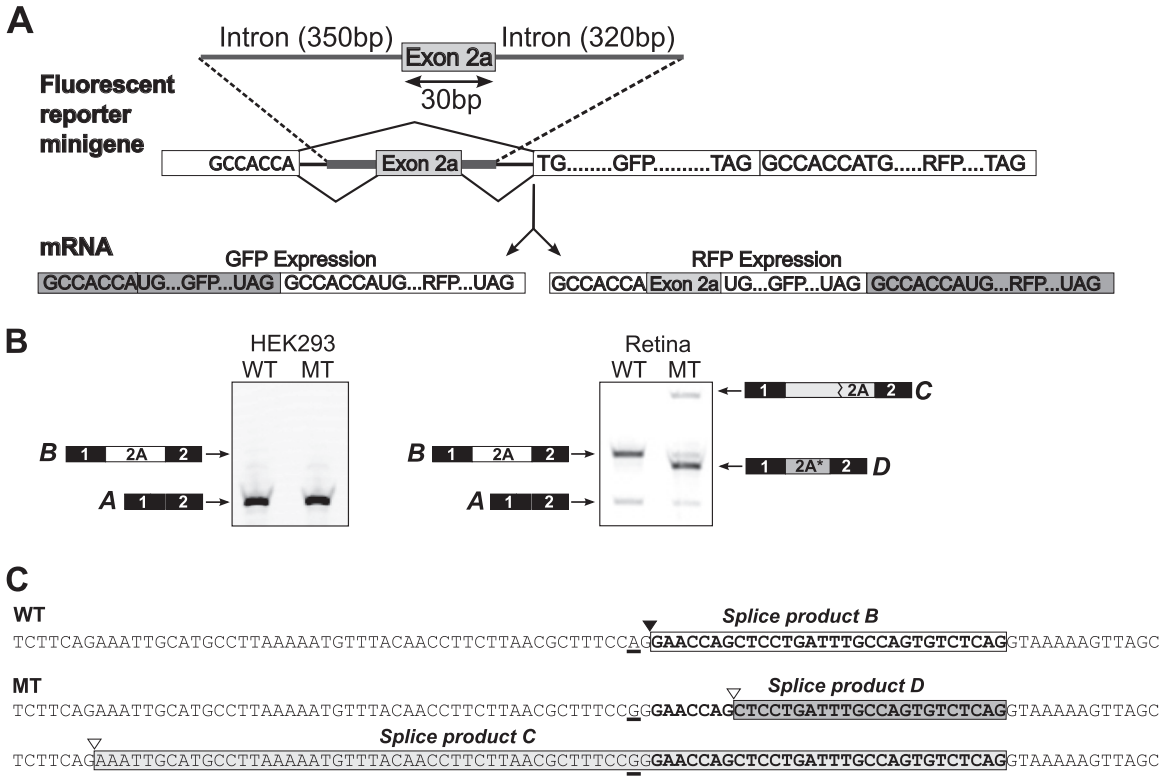

FIG 2 The *Bbs8* exon 2A minigene recapitulates the splicing of the full-length gene. (A) Schematic of the splicing minigene carrying mouse *Bbs8* exon 2A. The exon and portions of the flanking introns are cloned in the fluorescent reporter minigene (28). The ATG translation start codon of the GFP reading frame is split between the first and last exon of the minigene and is reconstituted when the alternative exon is spliced out. This leads to GFP expression, while the translation of the downstream RFP reading frame is suppressed. Inclusion of the alternative exon disrupts the ATG codon of the GFP reading frame, which blocks the GFP protein expression and simultaneously allows the downstream RFP reading frame to be translated. (B) RT-PCR analysis of the splicing of the wild-type (WT) and mutant (MT) exon 2A minigenes in HEK293 cells and mouse retina. HEK293 cells skip both the wild-type and mutant exon 2A from the mature transcripts (skipped isoform labeled A). In retina, wild-type exon 2A is included in the majority of transcripts. The major splice product of the mutant minigene, labeled D, is an inclusion of truncated exon that utilizes the same cryptic splice site as the exon in the context of the full-length human *BBS8* gene. A second high-molecular-weight splice product, labeled *C*, is derived from the use of a cryptic splice site upstream of exon 2A. (C) Sequence of mouse *Bbs8* exon 2A and portions of the adjacent introns. The mutation in the 3′ splice site is underlined. The exons included in the minigene mRNA (splice products *B*, *D*, and *C*) are boxed. A black arrowhead indicates the position of the wild-type 3′ splice site. White arrowheads indicate the positions of the cryptic 3′ and 5′ splice sites that are activated in the mutant minigene.

the retina of adult *Aipl1* and *Nrl* knockout mice strongly support the idea of photoreceptor-cell-specific splicing of this alternative exon.

To assess the BBS8L protein expression in the retina, we raised a rabbit polyclonal antibody against the peptide sequence encoded by exon 2A. Unfortunately, this BBS8L antibody was not suitable for immunolocalization in retinal sections. However, we were able to use the anti-exon 2A antibody to compare the levels of BBS8L expression in the retina from wild-type and *Aipl1* knockout animals by Western blotting. Wild-type retina expressed high levels of BBS8L protein that matched in mobility the recombinant BBS8L protein overexpressed in N2A cells, a mouse neuronal cell line (Fig. 1D). Consistent with the photoreceptor-cell-specific splicing of exon 2A, the BBS8L protein was undetectable in the retina lacking Aipl1 and in untransfected N2A cells. To determine the overall expression pattern of the BBS8S and BBS8L proteins in the retina, we probed the protein extracts with a commercially available pan-BBS8 antibody that recognizes both isoforms. Similarly to the results obtained with the BBS8L-specific antibody, the pan-BBS8 antibody detected high levels of BBS8L protein in the wild-type retina and no BBS8L protein in the retina from the *Aipl1* knockout mice. We also noticed that the retina lacking Aipl1 and the untransfected N2A cells expressed the shorter BBS8S protein, albeit at low levels. Overall, our results show that the BBS8L protein is expressed at high levels in photoreceptor cells.

The splice site mutation upstream of exon 2A results in cryptic splicing. The A-to-G substitution in the 3′ splice site of *BBS8* exon 2A (IVS1-2A>G) was postulated to cause nonsyndromic retinitis pigmentosa (RP) by preventing the inclusion of exon 2A in the mature transcripts (19). We established a reporter assay to test this hypothesis and to investigate the mechanism that controls the inclusion of exon 2A in *Bbs8*. This assay would also aid in visualizing the *Bbs8* exon 2A splicing event in a particular cell type in the retina. We cloned a 700-bp fragment containing the mouse exon 2A and portions of its flanking introns into a splicing reporter minigene under the control of ubiquitously active cytomegalovirus (CMV) promoter (Fig. 2A). In addition to the wild-type construct, we also created an exon 2A minigene carrying the IVS1-2A>G mutation. The splicing reporter is designed to produce red fluorescent protein (RFP) when exon 2A is included and green fluorescent protein (GFP) when the exon is skipped (28). This reporter construct allows us to use fluorescence microscopy

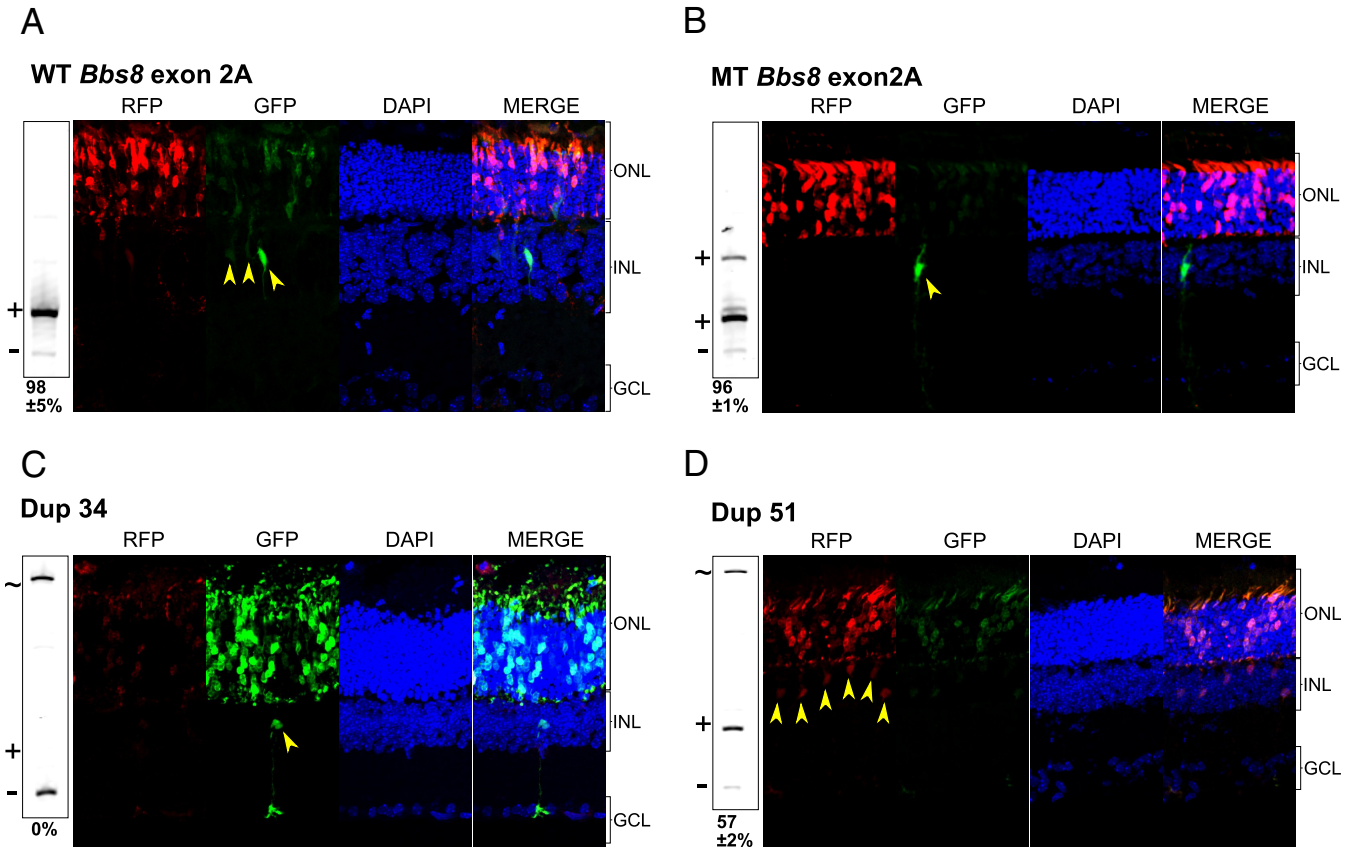

FIG 3 Photoreceptor-specific splicing of exon 2A in the context of the *Bbs8* minigene. Retinal sections from animals after electroporation with the indicated minigenes were imaged for GFP (green) and RFP (red). The nuclei are stained by DAPI (blue). ONL, INL, and GCL indicate the outer nuclear, inner nuclear, and ganglion cell layers, respectively. The RT-PCR analysis of minigene splicing in the retina is shown on the left. The percentage of exon inclusion ± standard error is shown under each gel image. (A) Wild-type exon 2A is included in photoreceptors as indicated by the high RFP expression observed on immunofluorescence and by RT-PCR analysis of total retinal RNA ("+" and "−" indicate exon inclusion and skipping, respectively). In contrast, higher GFP expression in the inner neurons demonstrates skipping of exon 2A in these cells (indicated by arrowheads). (B) Similarly to wild-type exon 2A, the exon-included products from mutant exon 2A are specifically detected in photoreceptors and not inner neurons. (C and D) The Dup34 (C) and Dup51 (D) exons show uniform fluorescent protein expression throughout the retina (bottom two panels; inner neurons are indicated by arrowheads). Both Dup34 and Dup51 produce unspliced RNA (indicated by "~" next to the RT-PCR gel). This unspliced RNA does not express RFP or GFP, because a small ORF in the downstream intron inhibits the translation of the downstream RFP reading frame (28).

to assess the inclusion of exon 2A by comparing RFP expression to GFP expression in individual cells. The splicing of exon 2A in the context of the minigene can also be quantified by RT-PCR using primers specific to the backbone.

We first analyzed the splicing of the wild-type and mutant exon 2A minigenes after transfecting them into human embryonic kidney (HEK293) tissue culture cells. Both minigenes produced mRNA that did not include exon 2A (Fig. 2B, product A). Next, we used subretinal injection and electroporation to introduce the *Bbs8* exon 2A minigenes into developing photoreceptor cells at P0 and analyzed their splicing by RT-PCR at P16 (30). We harvested retina at this time point because our results indicated that the inclusion of exon 2A is near its maximum at P16 (Fig. 1C). In addition, splicing of minigenes was visualized by fluorescence microscopy at P20 in retinas dissected from littermates of animals used for the RT-PCR experiments. Exon 2A was included in 98% of the minigene transcripts as determined by RT-PCR (Fig. 2B, product B). Surprisingly, introducing the 3′ splice site mutation into the minigene caused missplicing rather than exon skipping. Sequencing the PCR product showed that the shorter transcript is derived from the inclusion of a truncated 2A exon (represented as 2A*) due to the use of a cryptic 3′ splice site 7 nucleotides downstream of the normal acceptor site (Fig. 2B, product D). The minigene also produced two minor splice products, one migrating at a position significantly higher than wild-type exon 2A and one migrating at the same position as the wild-type exon. We determined by sequencing that the higher-molecular-weight splice product is generated by the use of a cryptic 3′ splice site upstream of exon 2A (product C). Splicing to both the intronic cryptic splice site (product C) and the exonic cryptic splice site (product D) is predicted to cause frameshift and premature termination of the Bbs8 reading frame in downstream exon 2.

Fluorescence microscopy imaging of the electroporated retinas showed that the electroporated minigenes were expressed mostly in photoreceptor cells, as very few inner neurons expressed the reporter fluorescent proteins (Fig. 3; see also Fig. S2 to S4 in the supplemental material). Thus, the RT-PCR signal was largely derived from the photoreceptor cells. In agreement with photoreceptor-cell-specific inclusion of exon 2A, we saw high levels of RFP expression in the photoreceptor outer nuclear layer (ONL)

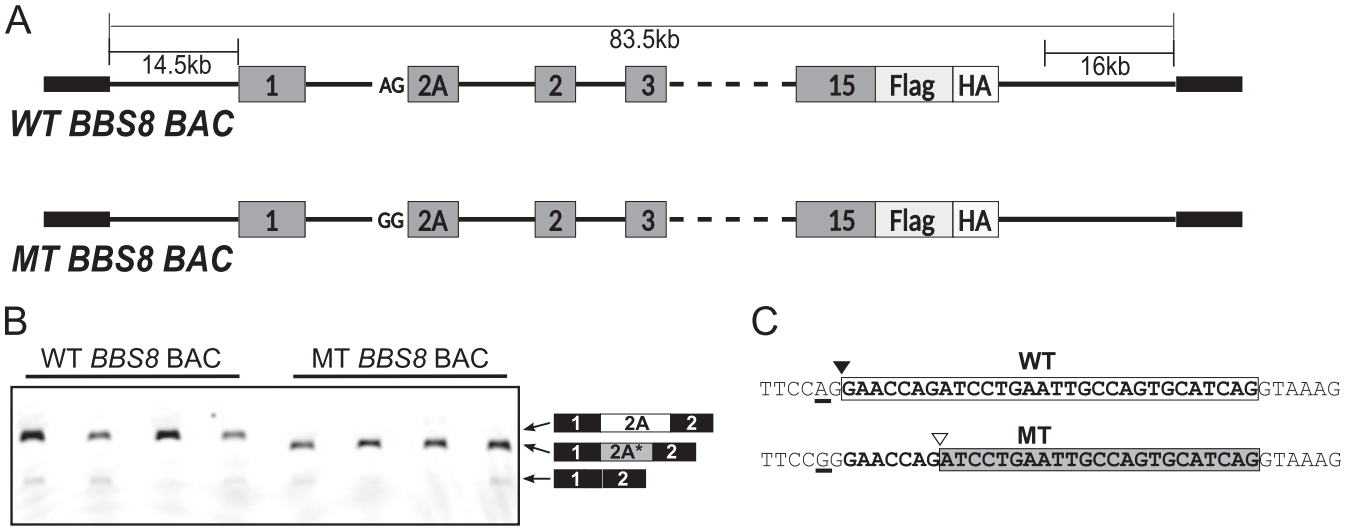

FIG 4 Inclusion of a truncated 2A exon in *BBS8* patient mutation linked to RP. (A) Schematic of the wild-type BAC clones containing the full-length human *BBS8* gene. The mutant BAC clone harbors an IVS1-2A>G mutation in the 3′ splice of exon 2A. (B) RT-PCR analysis of the splicing of the BAC transcripts in mouse retina at P16 after electroporation at P0 using primers specific to the human *BBS8* sequence. The wild-type BAC produces the exon 2A inclusion isoform of the mature *BBS8* mRNA. The mutation causes the inclusion of a shorter 2A* exon in the mature mRNAs. Also indicated on the right is the minor isoform that excludes exon 2A in retina electroporated with both wild-type and mutant *BBS8* BACs. (C) Genomic sequence of exon 2A and the adjacent introns showing the mutated splice site (underlines), the 3′ splice sites being used for the wild-type (black arrowhead), and the mutant exons (open arrowhead). The sequence of the exon being spliced is outlined with a white (wild type) or gray (mutant) box.

(Fig. 3A). Similar high RFP expression, which is indicative of exon inclusion, was observed with the minigene carrying the IVS1-2A>G mutation (Fig. 3B). To determine the exon 2A inclusion levels in inner neurons, we analyzed by fluorescence microscopy sections from animals electroporated with the exon 2A minigenes (Fig. 3A and B; see also Fig. S2 and S3). Invariably, the inner neurons displayed a high GFP-to-RFP ratio, which is indicative of skipping of exon 2A from the mature transcript (Fig. 3A, indicated with yellow arrowheads). Taking the data together, the fluorescence imaging of the mutant minigene in the retina and the results of the RT-PCR analysis show that the cryptic splice sites are used exclusively by the photoreceptor cells (Fig. 3B; see also Fig. S3). In contrast, inner neurons skip both the wild-type exon 2A and the mutant exon 2A altogether (Fig. 3A and B; see also Fig. S2 and S3).

To ensure that the observed splicing pattern is not influenced by the vector backbone, we electroporated two minigenes that carried synthetic alternative exons, Dup34 and Dup51, derived from the human β-globin gene (28). Dup34 is universally skipped, while Dup51 has an approximately 50% inclusion level in cultured cells (28, 32). We observed by RT-PCR and fluorescence microscopy that the Dup34 exon was completely skipped (high GFP expression) (Fig. 3C; see also Fig. S4 in the supplemental material) and the Dup51 exon was included at a high rate (high RFP expression) (Fig. 3D; see also Fig. S4). Neither of the two exons displayed a photoreceptor-specific splicing pattern.

We next examined the inclusion of exon 2A in the context of full-length introns and exons in the human *BBS8* gene. To do so, we used recombineering to modify a BAC clone containing the full-length human *BBS8* gene and created an A-to-G substitution in the 3′ splice site of exon 2A (Fig. 4A). The wild-type BAC and mutant BAC were then introduced into the developing photoreceptor cells of neonatal mice by subretinal injection and electroporation (30). The splicing of exon 2A in the retina was analyzed at P16 by RT-PCR using primers specific to the human sequence. We observed high levels of exon 2A inclusion in retina expressing the wild-type *BBS8* gene (Fig. 4B). Similarly to our minigene experiments, the IVS1-2A>G mutation did not cause skipping of exon 2A from the *BBS8* transcripts (Fig. 4B). Instead, the exon 2A isoform was replaced by an mRNA variant that included a slightly shorter exon. The shorter transcript contained a truncated 2A* exon with the use of the cryptic 3′ splice site 7 nucleotides downstream of the normal acceptor site, which we observed in our minigene experiments (Fig. 4C; see also Fig. S5 in the supplemental material).

Our results show that the molecular mechanism by which mutation of *Bbs8* exon 2A causes the loss of photoreceptor cells is missplicing leading to the inclusion of a truncated exon 2A rather than skipping of exon 2A.

The sequence of exon 2A does not direct its inclusion in photoreceptor cells. Our studies establish that *Bbs8* exon 2A is specifically included in photoreceptor cells. To determine how such specificity is achieved, we mapped the sequence elements that direct the splicing of exon 2A in photoreceptor cells. The sequence elements located within the exons (exonic splicing enhancers, or ESEs) are typically required for exon recognition and inclusion in the mature transcript (33–35). To determine if ESE sequences are involved in the photoreceptor-specific splicing of *Bbs8* exon 2A, we created four linker scanning minigenes (LS1 to LS4) in which overlapping 8-nucleotide segments of the exon were replaced with a PvuI linker sequence (Fig. 5A). To our surprise, all linker scanning mutants retained a high level of exon 2A inclusion in the retina (Fig. 5B). The LS1 mutant was the only one that showed a minor but significant decrease of approximately 14% in its inclusion level compared to the wild-type exon (Fig. 3A and 5B). We reasoned that, rather than carrying ESEs recognized by photoreceptor-specific splicing factors, *Bbs8* exon 2A might contain exonic splicing silencers (ESS) that repress its inclusion in other cell types. Alternatively, the linker sequence itself may contain an ESE.

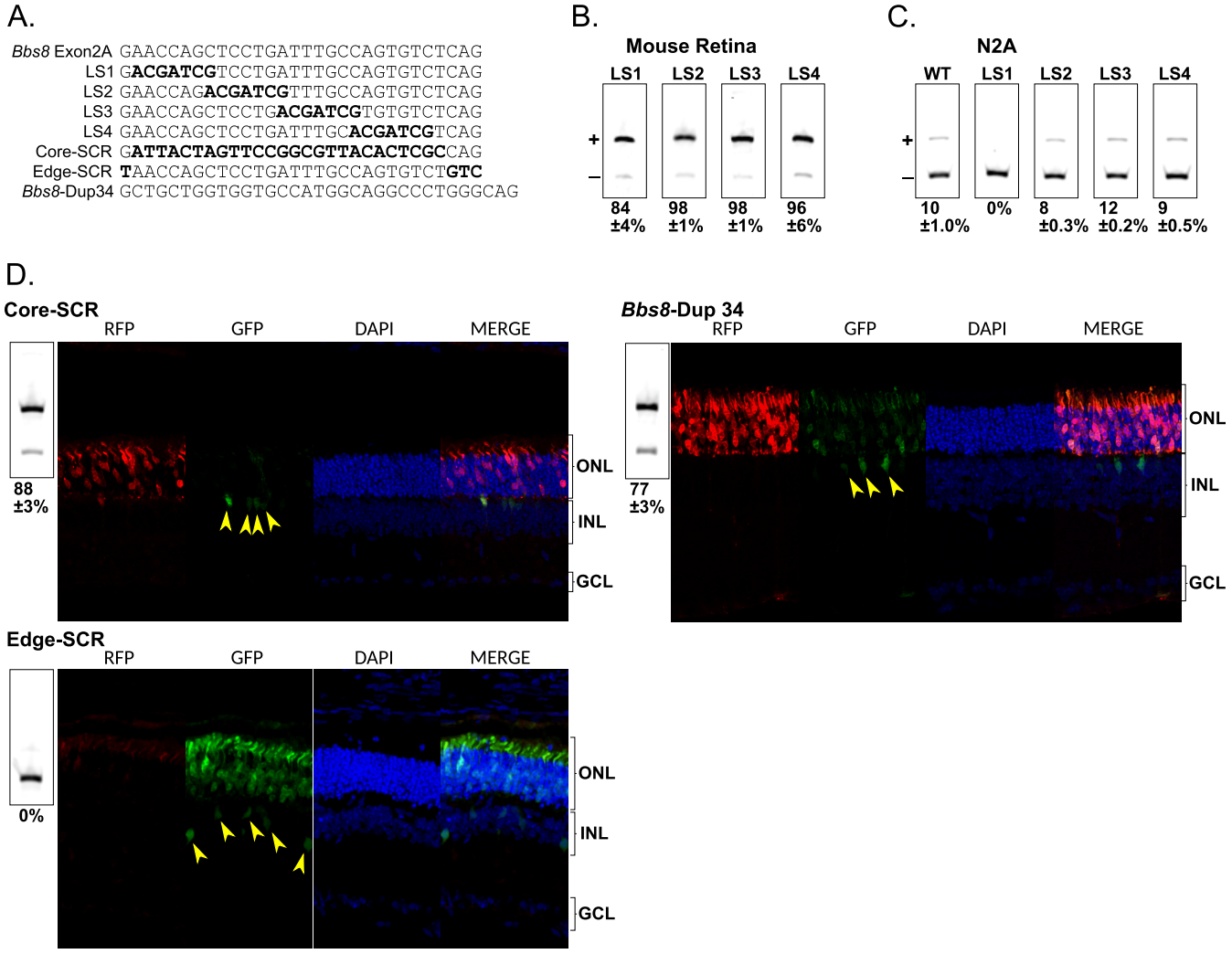

FIG 5 The sequence of *Bbs8* exon 2A does not control its splicing. (A) Sequences of the wild-type *Bbs8* exon 2A along with the sequences of the exon in mutant *Bbs8* minigenes. Four linker scanning mutants were created by replacing overlapping 8-nucleotide (nt) segments of the exon with a PvuI linker (the linker sequences is shown in bold). Two minigenes scramble the sequence of nucleotides 2 to 27 (Core-Scr) or mutate nucleotides 1, 28, 29, and 20 (Edge-Scr) of the *Bbs8* exon 2A. The mutated nucleotides are shown in bold. In *Bbs8*-Dup34, exon 2A is replaced by the Dup34 exon, while preserving the *Bbs8* introns. (B and C) RT-PCR analysis of the splicing of the linker scanning minigenes in the retina at postnatal day 16 (B) and in N2A cells at 48 h posttransfection (C). All linker scanning mutants are included at a high rate in the retina and skipped in N2A cells ("+" and "−" indicate exon inclusion and skipping, respectively). (D) RT-PCR (left panels) and fluorescence microscopy analysis (right panels) of the splicing of the Core-SCR, *Bbs8*-Dup34, and Edge-SCR minigenes in mouse retina. Each panel represents fluorescence microscopy images of the retinal sections accompanied by RT-PCR analysis of the minigene splicing. The percentage of exon inclusion ± standard error is shown under each gel image. The Core-SCR and *Bbs8*-Dup34 exons are included at a high rate in the photoreceptors and skipped from the minigene transcripts in the inner neurons (indicated by arrowheads). The Edge-SCR exon is skipped uniformly throughout the retina.

To test this hypothesis, we introduced the linker scanning mutants into N2A cells. In comparison to HEK293 cells where exon 2A was not included, we observed minor (10%) levels of wild-type (WT) exon 2A inclusion in N2A cells. However, this was significantly lower than the 98% inclusion levels in photoreceptor cells. We expected that mutants which disrupt ESS elements in exon 2A or add an ESE would increase its inclusion in the N2A cell line. We did not observe a significant increase in the exon 2A inclusion levels in any of the linker scanning mutations (Fig. 5C). As in our *in vivo* electroporation experiments, the LS1 mutant showed a minor but significant decrease in the exon 2A inclusion level (Fig. 5C).

To rule out the possibility that exon 2A contains redundant ESEs, we scrambled the exon 2A sequence (Core-SCR), while preserving the first and the last three nucleotides and the overall nucleotide composition (Fig. 5A). The first nucleotide and the last three nucleotides of the exon are part of the consensus splice site sequences and are directly contacted by the core spliceosome (36–38). By preserving these nucleotides in the Core-Scr minigene, we avoided disrupting interactions that are essential for splicing. The MaxEnt splice site scores for the 3′ splice sites of *Bbs8* exon 2A and Core-SCR are 8.82 and 8.61, respectively (39). The 5′ splice sites of both exons have a MaxEnt score of 8.59. We also created a minigene construct in which *Bbs8* exon 2A was substituted with the Dup34 exon, while preserving the *Bbs8* intronic sequence (Bbs8-Dup34). The MaxEnt score of the 3′ splice site of the Bbs8-Dup34 fusion (7.47) is lower but still represents a good match to the 3′ splice site consensus sequence. The 5′ splice site score of the Bbs8-

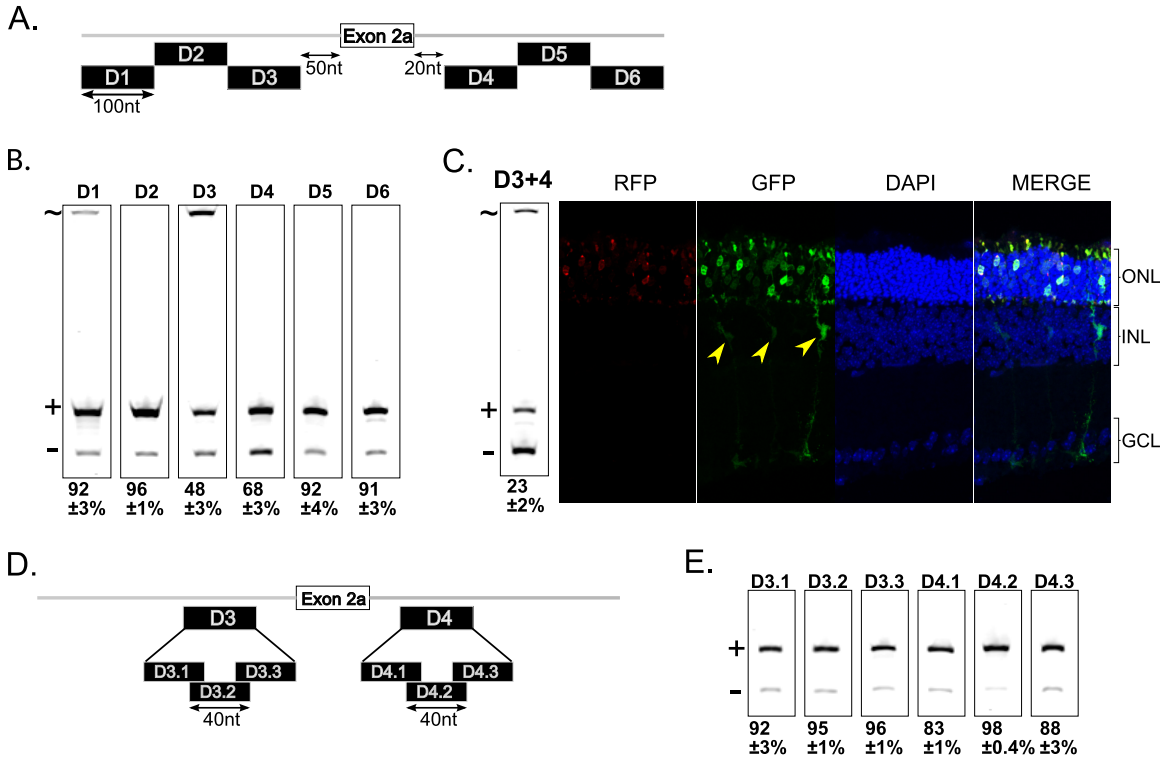

FIG 6 Intronic splicing enhancers promote exon 2A splicing in photoreceptor cells. (A) Schematic showing the positions of six 100-nt intronic deletions relative to *Bbs8* exon 2A. (B) RT-PCR analysis of the splicing of the intron deletion minigenes in mouse retina. The percentage of exon inclusion ± standard error is shown under each gel image. Most deletions, with exception of D3 and D4, do not affect significantly the splicing of *Bbs8* exon 2A. D3 and D4 cause a reduction of *Bbs8* exon inclusion ("+" and "−" indicate exon inclusion and skipping, respectively). In addition, the D3 mutant expresses significant amounts of mRNA which retains the upstream intron (indicated by "~"). The numbers under the gel images represent the percentages of the transcripts including the exon and the standard errors. (C) The simultaneous deletions of segments 3 and 4 reduce exon 2A inclusion levels in the retina to 23% (RT-PCR analysis gel shown on the left), which is accompanied by an increase of GFP expression and a reduction of RFP expression in the photoreceptor cells (right). The arrowheads point to an inner neuron. (D) Schematic showing the relative positions of six 40-nt deletions within the sequence of segments D3 and D4. (E) The 40-nt deletions shown on panel D do not alter *Bbs8* exon inclusion in the retina as detected by RT-PCR. The percentage of exon inclusion ± standard error is shown under each gel image.

Dup34 fusion is 8.59, identical to that of Bbs8 exon 2A and the Core-SCR. After subretinal injection and electroporation, both the Core-SCR and Bbs8-Dup34 minigenes displayed high levels of inclusion of the alternative exon: 88% and 77%, respectively (Fig. 5D; see also Fig. S6 and S7 in the supplemental material). Importantly, both exons were specifically included in photoreceptor cells and not in inner neurons (Fig. 5D). This result is in contrast to our previous observation where the Dup34 exon was completely skipped in photoreceptor cells when it was flanked by its original β-globin introns (Fig. 3C).

Mutating the first and last three nucleotides of Bbs8 exon 2A (Edge-SCR) to reduce the strength of the 3′ and 5′ splice sites to 6.17 and −8.27, respectively, completely abolished the inclusion of the exon (Fig. 5D; see also Fig. S8 in the supplemental material). Lack of exon 2A inclusion in this mutant is likely due to the disruption of the 5′ splice site, as indicated by its negative MaxEnt score.

The results from our mutagenesis study demonstrate that exon 2A does not contain splicing regulatory elements that are necessary for its inclusion in the photoreceptor cells and that the *cis* elements that control *Bbs8* exon 2A splicing are likely intronic.

Redundant intronic splicing enhancers (ISEs) regulate the splicing of *Bbs8* exon 2A. To map the regulatory elements in the introns flanking Bbs8 exon 2A, we created six deletion mutants, each one removing 100 nucleotides from the upstream and downstream introns cloned in the exon 2A minigene (Fig. 6A). In all the deletions, we preserved the sequences of the 3′ and 5′ splice sites, and the putative branch point, which are recognized by the core spliceosome. We observed that deletion of the segments adjacent to the exon, labeled D3 and D4 (D3/D4), resulted in significant reduction of exon 2A inclusion in the retina (Fig. 3A and 6B). Additionally, the deletion of segment D3 caused retention of the upstream intron in part of the mature transcripts. The remaining four deletions had a minimal effect or no effect on the exon 2A inclusion levels or the splicing efficiency of the introns. Combined deletions of segments D3 and D4 dramatically reduced the exon 2A inclusion level in photoreceptor cells from 98% (Fig. 2) to 23% (Fig. 6C; see also Fig. S9 in the supplemental material). In agreement with the decrease in the inclusion levels of exon 2A in the D3/D4 deletion, we saw increased expression of GFP in photoreceptor cells (Fig. 6C). This is in contrast to our earlier result, with intact exon 2A introns showing robust expression of RFP (Fig. 3D). Altogether, these findings indicate that ISE elements located in both the D3 and D4 segments promote in concert the splicing of exon 2A in photoreceptor cells.

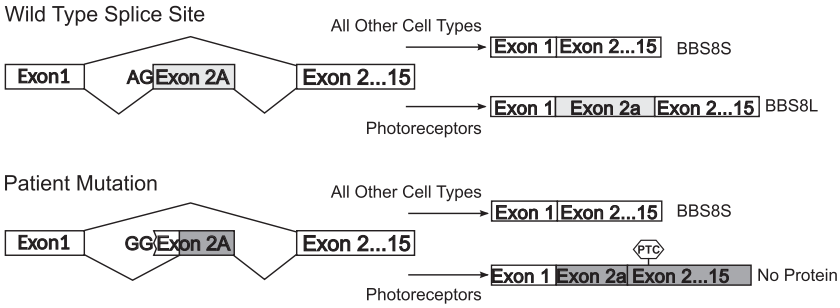

FIG 7 Model explaining the confinement of the phenotype of the *BBS8* IVS1-2A>G mutation to photoreceptor cells. *BBS8* exon 2A is included specifically in the photoreceptor cells to produce BBS8L protein. All other cell types skip exon 2A and produce the shorter BBS8S protein. Disruption of the exon 2A splice site by the IVS1-2A>G mutation causes the use of a cryptic splice site, resulting in a frameshift. As a result of the frameshift, the *BBS8* reading frame ends with a premature termination codon (PTC) in exon 2. As BBS8L is the exclusive isoform in photoreceptors, the mutation ultimately results in elimination of the BBS8 protein from this cell type. All other cell types are immune to the mutation as they skip exon 2A and do not utilize the cryptic splice site.

To obtain a higher-resolution map of the ISEs controlling exon 2A splicing, we generated six additional mutants that had overlapping 40-nucleotide deletions in segments D3 and D4 (Fig. 6D). We did not observe any significant changes in the levels of exon 2A inclusion in any of the shorter deletion mutants (Fig. 6E). We conclude that segments D3 and D4 contain multiple redundant ISEs, so that the deletion of any single ISE is insufficient to significantly impact the splicing of exon 2A.

DISCUSSION

The lack of cellular models and the technical difficulty of analyzing the gene expression profiles of individual cell subtypes in the retina have presented significant obstacles to studying the regulation of gene expression and alternative splicing in photoreceptor cells. Here we demonstrate that these obstacles can be overcome by using genetically engineered mouse models to identify photoreceptor-specific transcripts and subretinal injection and electroporation to dissect the regulation of their expression. In particular, the use of the fluorescent splicing reporter allowed us to visualize the splicing regulation of *Bbs8* exon 2A in individual retinal cells. As the fluorescent reporter minigene is designed to accommodate most alternative exons, our approach is generally applicable to studying splicing *in vivo*.

To our surprise, the IVS1-2A>G mutation in the splice acceptor site of *Bbs8* exon 2A does not cause skipping of the exon, which in turn would result in the expression of the BBS8S protein in place of the photoreceptor-specific BBS8L. Instead, the mutation forced the use of a cryptic splice site located 7 nt downstream of the mutated site. The splicing of mutant exon 2A is consistent with our finding that any exon placed in the context of the introns flanking *Bbs8* exon 2A is spliced efficiently in photoreceptor cells as long as it carries functional splice sites. On the basis of the splicing pattern of mutant exon 2A, we propose that the disease mechanism involves missplicing, which in turn results in premature termination of the *BBS8* reading frame and elimination of the BBS8 protein in photoreceptors (Fig. 7). In this scenario, we expect no BBS8 protein (BBS8L or BBS8S) expression in photoreceptor cells. This is akin to generating a photoreceptor-specific BBS8 knockout. Our attempts to detect BBS8 protein expression in the retina from either the wild-type or mutant BAC constructs were not fruitful. This was likely due to the low efficiency of the BAC electroporation. A robust test to examine the effect of the IVS1-2A>G mutation on BBS8 protein synthesis will require animal models in which the mutation is introduced in the endogenous *Bbs8* locus or in transgenes carrying the BAC constructs described here and bred into a *Bbs8* null animal(s).

How is the phenotype of the IVS1-2A>G mutation confined to photoreceptors? All the cell types other than photoreceptor cells that we have tested skip exon 2A and consequently do not utilize the cryptic splice sites. These cells express the short BBS8 isoform (BBS8S) and are immune to the mutation (Fig. 7). Thus, the phenotype of the IVS1-2A>G mutation is determined by the photoreceptor-specific alternative splicing program. To our knowledge, such an interaction between tissue-specific alternative splicing and genetic mutations has been described only in Stickler syndrome. Stickler syndrome is caused by mutations in at least 4 collagen genes and presents as a systemic disorder characterized by facial and eye abnormalities, hearing loss, and joint problems (40, 41). However, mutations in exon 2 of the COL2A1 gene but not in other exons of the same gene predominantly produce an eye phenotype due to the tissue-specific splicing of this exon (42–45). We are tempted to speculate that the BBS8 IVS1-2A>G and COL2A1 exon 2 mutations may not be isolated cases. Neurons, epithelial cells, and muscle cells express highly cell-type-specific splicing regulators and consequently present characteristic splicing programs. Furthermore, splicing regulatory sequences are a rich and often underappreciated target for disease-causing genetic mutations (46). Approximately 10% of disease-causing mutations disrupt the canonical splice site, and an additional 25% are estimated to affect splicing regulatory sequences within the exons (47, 48). Thus, we expect the phenotype of many disease-causing mutations to be modulated by the alternative splicing machinery.

Bbs8 exon 2A is highly photoreceptor specific, with nearly 100% inclusion levels in photoreceptor cells, while it is not included or is included at very low levels outside the retina. After exhaustive mutagenesis, we found that efficient splicing of *Bbs8* exon 2A in photoreceptor cells does not depend on ESEs. Strikingly, even the randomized sequence of the Core-SCR exon and that of the unrelated Dup34 exon were spliced efficiently in photoreceptor cells as long as they were in the context of the introns flanking *Bbs8* exon 2A. Two 100-nucleotide segments, D3 located upstream and D4 located downstream of exon 2A, work in concert to promote inclusion of exon 2A in photoreceptors. The D3 and D4 segments are likely composed of multiple redundant intronic splicing enhancers, as a series of shorter deletions did not significantly reduce the efficiency of exon 2A splicing. Intronic splicing

regulatory elements have a well-established role in regulating alternative splicing and promoting alternative exon splicing in specific tissues and cell types. In particular, neuronal and muscle-specific microexons are characterized by a high degree of conservation of the adjacent intronic sequences compared to longer exons with similar tissue-specific regulation (49, 50). The intron sequence conservation in these exons is dictated by the presence of regulatory sequences that are recognized by Rbfox1/2/3, PTBP1/2, and SRRM4 splicing regulators (49, 50).

At present, we do not know the identity of the *trans*-acting factors that bind to the intronic splicing enhancers flanking *Bbs8* exon 2A to promote its inclusion in photoreceptor cells. We are also unaware of any RNA binding proteins that are specifically expressed in photoreceptors. Several genome-wide studies have provided evidence that the retina expresses a highly diverse set of alternative transcripts that are developmentally regulated (51–54). It is unclear to what degree the retina-specific transcript variants identified in these studies are derived from photoreceptor cells. We believe that, by expanding it to the genomic scale, our approach of comparing the expression levels in the retina of Aipl1 knockout mice to those in the retina of wild-type animals will make it possible to identify the splicing regulators and alternative transcripts specific to the photoreceptor cells. In the absence of photoreceptor-specific proteins that directly bind to the *Bbs8* pre-mRNA, the splicing of the exon 2A may be controlled by a combination of otherwise ubiquitously expressed splicing factors that is unique to this cell type. Such a mode of regulation would be consistent with the combinatorial nature of the mechanisms controlling alternative splicing (55–57).

ACKNOWLEDGMENTS

We thank Anand Swaroop for generously providing the Nrl knockout animal used in this study. We thank Peter Mathers and Helen Rodgers for providing RNA samples from embryonic and early postnatal mouse retinas and the anti-Chx and anti-Pax6 antibodies. We thank Maxim Sokolov and Marycharmain Belcastro for the *Gnat1* qPCR primers and the anti-Pdc antibody. We appreciate the constructive criticisms received from Lisa Salati, Maxim Sokolov, Peter Mathers, and Mike Schaller (West Virginia University) and Shalini Sharma (University of Arizona).

Imaging experiments were performed in the West Virginia University Microscope Imaging Facility, which has been supported by the Mary Babb Randolph Cancer Center and NIH grants P20 RR016440, P30 GM103488, and P20 GM103434. This work was supported by grants from the National Institutes of Health (EY017035), West Virginia Lions, and Lions Club International Fund and by an internal grant from West Virginia University.

We declare that we have no conflicts of interest.

REFERENCES

1. **Wei Q, Zhang Y, Li Y, Zhang Q, Ling K, Hu J.** 2012. The BBSome controls IFT assembly and turnaround in cilia. Nat Cell Biol **14:**950–957. http://dx.doi.org/10.1038/ncb2560.
2. **Seo S, Zhang Q, Bugge K, Breslow DK, Searby CC, Nachury MV, Sheffield VC.** 2011. A novel protein LZTFL1 regulates ciliary trafficking of the BBSome and Smoothened. PLoS Genet **7:**e1002358. http://dx.doi.org/10.1371/journal.pgen.1002358.
3. **Domire JS, Green JA, Lee KG, Johnson AD, Askwith CC, Mykytyn K.** 2011. Dopamine receptor 1 localizes to neuronal cilia in a dynamic process that requires the Bardet-Biedl syndrome proteins. Cell Mol Life Sci **68:**2951–2960. http://dx.doi.org/10.1007/s00018-010-0603-4.
4. **Lechtreck K-F, Johnson EC, Sakai T, Cochran D, Ballif BA, Rush J, Pazour GJ, Ikebe M, Witman GB.** 2009. The Chlamydomonas reinhardtii BBSome is an IFT cargo required for export of specific signaling proteins from flagella. J Cell Biol **187:**1117–1132. http://dx.doi.org/10.1083/jcb.200909183.
5. **Berbari NF, Lewis JS, Bishop GA, Askwith CC, Mykytyn K.** 2008. Bardet-Biedl syndrome proteins are required for the localization of G protein-coupled receptors to primary cilia. Proc Natl Acad Sci U S A **105:**4242–4246. http://dx.doi.org/10.1073/pnas.0711027105.
6. **Su X, Driscoll K, Yao G, Raed A, Wu M, Beales PL, Zhou J.** 2014. Bardet-Biedl syndrome proteins 1 and 3 regulate the ciliary trafficking of polycystic kidney disease 1 protein. Hum Mol Genet **23:**5441–5451. http://dx.doi.org/10.1093/hmg/ddu267.
7. **Ansley SJ, Badano JL, Blacque OE, Hill J, Hoskins BE, Leitch CC, Chul Kim J, Ross AJ, Eichers ER, Teslovich TM, Mah AK, Johnsen RC, Cavender JC, Alan Lewis R, Leroux MR, Beales PL, Katsanis N.** 2003. Basal body dysfunction is a likely cause of pleiotropic Bardet-Biedl syndrome. Nature **425:**628–633. http://dx.doi.org/10.1038/nature02030.
8. **Sung C-H, Leroux MR.** 2013. The roles of evolutionarily conserved functional modules in cilia-related trafficking. Nat Cell Biol **15:**1387–1397. http://dx.doi.org/10.1038/ncb2888.
9. **Barbelanne M, Hossain D, Chan DP, Peränen J, Tsang WY.** 30 December 2014, posting date. Nephrocystin proteins NPHP5 and Cep290 regulate BBSome integrity, ciliary trafficking and cargo delivery. Hum Mol Genet http://dx.doi.org/10.1093/hmg/ddu738.
10. **Zaghloul NA, Katsanis N.** 2009. Mechanistic insights into Bardet-Biedl syndrome, a model ciliopathy. J Clin Invest **119:**428–437. http://dx.doi.org/10.1172/JCI37041.
11. **M'hamdi O, Ouertani I, Chaabouni-Bouhamed H.** 2014. Update on the genetics of Bardet-Biedl syndrome. Mol Syndromol **5:**51–56. http://dx.doi.org/10.1159/000357054.
12. **Nishimura DY, Fath M, Mullins RF, Searby C, Andrews M, Davis R, Andorf JL, Mykytyn K, Swiderski RE, Yang B, Carmi R, Stone EM, Sheffield VC.** 2004. Bbs2-null mice have neurosensory deficits, a defect in social dominance, and retinopathy associated with mislocalization of rhodopsin. Proc Natl Acad Sci U S A **101:**16588–16593. http://dx.doi.org/10.1073/pnas.0405496101.
13. **Abd-El-Barr MM, Sykoudis K, Andrabi S, Eichers ER, Pennesi ME, Tan PL, Wilson JH, Katsanis N, Lupski JR, Wu SM.** 2007. Impaired photoreceptor protein transport and synaptic transmission in a mouse model of Bardet-Biedl syndrome. Vision Res **47:**3394–3407. http://dx.doi.org/10.1016/j.visres.2007.09.016.
14. **Aldahmesh MA, Abu Safieh L, Alkuraya H, Al-Rajhi A, Shamseldin H, Hashem M, Alzahrani F, Khan AO, Alqahtani F, Rahbeeni Z, Alowain M, Khalak H, Al-Hazzaa S, Meyer BF, Alkuraya FS.** 2009. Molecular characterization of retinitis pigmentosa in Saudi Arabia. Mol Vis **15:**2464–2469.
15. **Estrada-Cuzcano A, Koenekoop RK, Senechal A, De Baere EB, de Ravel T, Banfi S, Kohl S, Ayuso C, Sharon D, Hoyng CB, Hamel CP, Leroy BP, Ziviello C, Lopez I, Bazinet A, Wissinger B, Sliesoraityte I, Avila-Fernandez A, Littink KW, Vingolo EM, Signorini S, Banin E, Mizrahi-Meissonnier L, Zrenner E, Kellner U, Collin RW, den Hollander AI, Cremers FP, Klevering BJ.** 2012. BBs1 mutations in a wide spectrum of phenotypes ranging from nonsyndromic retinitis pigmentosa to Bardet-Biedl syndrome. Arch Ophthalmol **130:**1425–1432. http://dx.doi.org/10.1001/archophthalmol.2012.2434.
16. **Abu Safieh L, Aldahmesh MA, Shamseldin H, Hashem M, Shaheen R, Alkuraya H, Al Hazzaa SA, Al-Rajhi A, Alkuraya FS.** 2010. Clinical and molecular characterisation of Bardet-Biedl syndrome in consanguineous populations: the power of homozygosity mapping. J Med Genet **47:**236–241. http://dx.doi.org/10.1136/jmg.2009.070755.
17. **Fan Y, Esmail MA, Ansley SJ, Blacque OE, Boroevich K, Ross AJ, Moore SJ, Badano JL, May-Simera H, Compton DS, Green JS, Lewis RA, van Haelst MM, Parfrey PS, Baillie DL, Beales PL, Katsanis N, Davidson WS, Leroux MR.** 2004. Mutations in a member of the Ras superfamily of small GTP-binding proteins causes Bardet-Biedl syndrome. Nat Genet **36:**989–993. http://dx.doi.org/10.1038/ng1414.
18. **Stoetzel C, Laurier V, Faivre L, Mégarbané A, Perrin-Schmitt F, Verloes A, Bonneau D, Mandel J-L, Cossee M, Dollfus H.** 2006. BBS8 is rarely mutated in a cohort of 128 Bardet-Biedl syndrome families. J Hum Genet **51:**81–84. http://dx.doi.org/10.1007/s10038-005-0320-2.
19. **Riazuddin SA, Iqbal M, Wang Y, Masuda T, Chen Y, Bowne S, Sullivan LS, Waseem NH, Bhattacharya S, Daiger SP, Zhang K, Khan SN, Riazuddin S, Hejtmancik JF, Sieving PA, Zack DJ, Katsanis N.** 2010. A splice-site mutation in a retina-specific exon of BBS8 causes nonsyn-

dromic retinitis pigmentosa. Am J Hum Genet **86:**805–812. http://dx.doi.org/10.1016/j.ajhg.2010.04.001.
20. **Pretorius PR, Baye LM, Nishimura DY, Searby CC, Bugge K, Yang B, Mullins RF, Stone EM, Sheffield VC, Slusarski DC.** 2010. Identification and functional analysis of the vision-specific BBS3 (ARL6) long isoform. PLoS Genet **6:**e1000884. http://dx.doi.org/10.1371/journal.pgen.1000884.
21. **Pretorius PR, Aldahmesh MA, Alkuraya FS, Sheffield VC, Slusarski DC.** 2011. Functional analysis of BBS3 A89V that results in non-syndromic retinal degeneration. Hum Mol Genet **20:**1625–1632. http://dx.doi.org/10.1093/hmg/ddr039.
22. **May-Simera HL, Petralia RS, Montcouquiol M, Wang Y-X, Szarama KB, Liu Y, Lin W, Deans MR, Pazour GJ, Kelley MW.** 2015. Ciliary proteins Bbs8 and Ift20 promote planar cell polarity in the cochlea. Development **142:**555–566. http://dx.doi.org/10.1242/dev.113696.
23. **Bin J, Madhavan J, Ferrini W, Mok CA, Billingsley G, Héon E.** 2009. BBS7 and TTC8 (BBS8) mutations play a minor role in the mutational load of Bardet-Biedl syndrome in a multiethnic population. Hum Mutat **30:**E737–E746. http://dx.doi.org/10.1002/humu.21040.
24. **Hichri H, Stoetzel C, Laurier V, Caron S, Sigaudy S, Sarda P, Hamel C, Martin-Coignard D, Gilles M, Leheup B, Holder M, Kaplan J, Bitoun P, Lacombe D, Verloes A, Bonneau D, Perrin-Schmitt F, Brandt C, Besancon A-F, Mandel J-L, Cossée M, Dollfus H.** 2005. Testing for triallelism: analysis of six BBS genes in a Bardet-Biedl syndrome family cohort. Eur J Hum Genet **13:**607–616. http://dx.doi.org/10.1038/sj.ejhg.5201372.
25. **Ramamurthy V, Niemi GA, Reh TA, Hurley JB.** 2004. Leber congenital amaurosis linked to AIPL1: a mouse model reveals destabilization of cGMP phosphodiesterase. Proc Natl Acad Sci U S A **101:**13897–13902. http://dx.doi.org/10.1073/pnas.0404197101.
26. **Mears AJ, Kondo M, Swain PK, Takada Y, Bush RA, Saunders TL, Sieving PA, Swaroop A.** 2001. Nrl is required for rod photoreceptor development. Nat Genet **29:**447–452. http://dx.doi.org/10.1038/ng774.
27. **Percifield R, Murphy D, Stoilov P.** 2014. Medium throughput analysis of alternative splicing by fluorescently labeled RT-PCR. Methods Mol Biol **1126:**299–313. http://dx.doi.org/10.1007/978-1-62703-980-2_22.
28. **Stoilov P, Lin C-H, Damoiseaux R, Nikolic J, Black DL.** 2008. A high-throughput screening strategy identifies cardiotonic steroids as alternative splicing modulators. Proc Natl Acad Sci U S A **105:**11218–11223. http://dx.doi.org/10.1073/pnas.0801661105.
29. **Copeland NG, Jenkins NA, Court DL.** 2001. Recombineering: a powerful new tool for mouse functional genomics. Nat Rev Genet **2:**769–779. http://dx.doi.org/10.1038/35093556.
30. **Matsuda T, Cepko CL.** 2004. Electroporation and RNA interference in the rodent retina in vivo and in vitro. Proc Natl Acad Sci U S A **101:**16–22. http://dx.doi.org/10.1073/pnas.2235688100.
31. **Swaroop A, Kim D, Forrest D.** 2010. Transcriptional regulation of photoreceptor development and homeostasis in the mammalian retina. Nat Rev Neurosci **11:**563–576. http://dx.doi.org/10.1038/nrn2880.
32. **Modafferi EF, Black DL.** 1997. A complex intronic splicing enhancer from the c-src pre-mRNA activates inclusion of a heterologous exon. Mol Cell Biol **17:**6537–6545.
33. **Blencowe BJ.** 2000. Exonic splicing enhancers: mechanism of action, diversity and role in human genetic diseases. Trends Biochem Sci **25:**106–110. http://dx.doi.org/10.1016/S0968-0004(00)01549-8.
34. **Matlin AJ, Clark F, Smith CWJ.** 2005. Understanding alternative splicing: towards a cellular code. Nat Rev Mol Cell Biol **6:**386–398. http://dx.doi.org/10.1038/nrm1645.
35. **Black DL.** 2003. Mechanisms of alternative pre-messenger RNA splicing. Annu Rev Biochem **72:**291–336. http://dx.doi.org/10.1146/annurev.biochem.72.121801.161720.
36. **Wu S, Romfo CM, Nilsen TW, Green MR.** 1999. Functional recognition of the 3′ splice site AG by the splicing factor U2AF35. Nature **402:**832–835. http://dx.doi.org/10.1038/45590.
37. **Séraphin B, Kretzner L, Rosbash M.** 1988. A U1 snRNA:pre-mRNA base pairing interaction is required early in yeast spliceosome assembly but does not uniquely define the 5′ cleavage site. EMBO J **7:**2533–2538.
38. **Malca H, Shomron N, Ast G.** 2003. The U1 snRNP base pairs with the 5′ splice site within a penta-snRNP complex. Mol Cell Biol **23:**3442–3455. http://dx.doi.org/10.1128/MCB.23.10.3442-3455.2003.
39. **Yeo G, Burge CB.** 2004. Maximum entropy modeling of short sequence motifs with applications to RNA splicing signals. J Comput Biol **11:**377–394. http://dx.doi.org/10.1089/1066527041410418.
40. **Stickler GB, Belau PG, Farrell FJ, Jones JD, Pugh DG, Steinberg AG, Ward LE.** 1965. Hereditary progressive arthro-ophthalmopathy. Mayo Clin Proc **40:**433–455.
41. **Stickler GB, Hughes W, Houchin P.** 2001. Clinical features of hereditary progressive arthro-ophthalmopathy (Stickler syndrome): a survey. Genet Med **3:**192–196. http://dx.doi.org/10.1097/00125817-200105000-00008.
42. **Bishop PN, Reardon AJ, Mcleod D, Ayad S.** 1994. Identification of alternatively spliced variants of type II procollagen in vitreous. Biochem Biophys Res Commun **203:**289–295. http://dx.doi.org/10.1006/bbrc.1994.2180.
43. **Lui VCH, Ng LJ, Nicholls J, Tam PPL, Cheah KSE.** 1995. Tissue-specific and differential expression of alternatively spliced α1(II) collagen mRNAs in early human embryos. Dev Dyn **203:**198–211. http://dx.doi.org/10.1002/aja.1002030208.
44. **Sandell LJ, Nalin AM, Reife RA.** 1994. Alternative splice form of type II procollagen mRNA (IIA) is predominant in skeletal precursors and noncartilaginous tissues during early mouse development. Dev Dyn **199:**129–140. http://dx.doi.org/10.1002/aja.1001990206.
45. **Donoso LA, Edwards AO, Frost AT, Ritter R, III, Ahmad N, Vrabec T, Rogers J, Meyer D, Parma S.** 2003. Clinical variability of Stickler syndrome: role of exon 2 of the collagen COL2A1 gene. Surv Ophthalmol **48:**191–203. http://dx.doi.org/10.1016/S0039-6257(02)00460-5.
46. **López-Bigas N, Audit B, Ouzounis C, Parra G, Guigó R.** 2005. Are splicing mutations the most frequent cause of hereditary disease? FEBS Lett **579:**1900–1903. http://dx.doi.org/10.1016/j.febslet.2005.02.047.
47. **Sterne-Weiler T, Howard J, Mort M, Cooper DN, Sanford JR.** 2011. Loss of exon identity is a common mechanism of human inherited disease. Genome Res **21:**1563–1571. http://dx.doi.org/10.1101/gr.118638.110.
48. **Krawczak M, Thomas NST, Hundrieser B, Mort M, Wittig M, Hampe J, Cooper DN.** 2007. Single base-pair substitutions in exon–intron junctions of human genes: nature, distribution, and consequences for mRNA splicing. Hum Mutat **28:**150–158. http://dx.doi.org/10.1002/humu.20400.
49. **Irimia M, Weatheritt RJ, Ellis JD, Parikshak NN, Gonatopoulos-Pournatzis T, Babor M, Quesnel-Vallières M, Tapial J, Raj B, O'Hanlon D, Barrios-Rodiles M, Sternberg MJE, Cordes SP, Roth FP, Wrana JL, Geschwind DH, Blencowe BJ.** 2014. A highly conserved program of neuronal microexons is misregulated in autistic brains. Cell **159:**1511–1523. http://dx.doi.org/10.1016/j.cell.2014.11.035.
50. **Li YI, Sanchez-Pulido L, Haerty W, Ponting CP.** 18 December 2014, posting date. RBFOX and PTBP1 proteins regulate the alternative splicing of micro-exons in human brain transcripts. Genome Res http://dx.doi.org/10.1101/gr.181990.114.
51. **Farkas MH, Grant GR, White JA, Sousa ME, Consugar MB, Pierce EA.** 2013. Transcriptome analyses of the human retina identify unprecedented transcript diversity and 3.5 Mb of novel transcribed sequence via significant alternative splicing and novel genes. BMC Genomics **14:**486. http://dx.doi.org/10.1186/1471-2164-14-486.
52. **Hackam AS, Qian J, Liu D, Gunatilaka T, Farkas RH, Chowers I, Kageyama M, Parmigiani G, Zack DJ.** 2004. Comparative gene expression analysis of murine retina and brain. Mol Vis **10:**637–649.
53. **Wan J, Masuda T, Hackler L, Torres KM, Merbs SL, Zack DJ, Qian J.** 2011. Dynamic usage of alternative splicing exons during mouse retina development. Nucleic Acids Res **39:**7920–7930. http://dx.doi.org/10.1093/nar/gkr545.
54. **Gamsiz ED, Ouyang Q, Schmidt M, Nagpal S, Morrow EM.** 2012. Genome-wide transcriptome analysis in murine neural retina using high-throughput RNA sequencing. Genomics **99:**44–51. http://dx.doi.org/10.1016/j.ygeno.2011.09.003.
55. **Hertel KJ.** 2008. Combinatorial control of exon recognition. J Biol Chem **283:**1211–1215. http://dx.doi.org/10.1074/jbc.R700035200.
56. **Modafferi EF, Black DL.** 1999. Combinatorial control of a neuron-specific exon. RNA **5:**687–706. http://dx.doi.org/10.1017/S1355838299990155.
57. **Singh NN, Androphy EJ, Singh RN.** 2004. In vivo selection reveals combinatorial controls that define a critical exon in the spinal muscular atrophy genes. RNA **10:**1291–1305. http://dx.doi.org/10.1261/rna.7580704.